International Journal of Design & Nature and Ecodynamics
Vol. 21, No. 2, February, 2026, pp. 577-583
Journal homepage: http://iieta.org/journals/ijdne

Candidates Enhanced Ballistic Performance of Polyurethane Composites Reinforced with Graphite-Derived Graphene

Surya Pranowo[1], Maming[2], Abdul Karim[2], Bulkis Musa[2], Wildan Mubaraq[2], Rizal Irfandi[3], Erna Mayasari[2], Indah Raya[2*]

[1] Laboratorium of Forensic, South Sulawesi Regional Police Laboratory, Makassar 90241, Indonesia
[2] Department of Chemistry, Faculty of Mathematics and Natural Science, Hasanuddin University, Makassar 90245, Indonesia
[3] Department of Chemistry, Faculty of Mathematics and Natural Science, Universitas Negeri Makassar, Makassar 90244, Indonesia

Corresponding Author Email: indahraya@unhas.ac.id

https://doi.org/10.18280/ijdne.210226

Received: 13 December 2025
Revised: 27 January 2026
Accepted: 13 February 2026
Available online: 28 February 2026

Keywords:
synthesis, graphite, graphene, polyethylene, military bulletproof

ABSTRACT

Graphene oxide (GO) was synthesized from commercial graphite using a modified Hummers method and subsequently reduced with Zn powder to obtain reduced graphene oxide (rGO). The rGO was incorporated into a polyurethane matrix to fabricate lightweight, ballistic-resistant composites. Structural characterization by Fourier Transform Infrared (FTIR), X-Ray Diffraction (XRD), and Scanning Electron Microscopy–Energy-Dispersive X-ray Spectroscopy (SEM–EDX) confirmed the successful reduction of GO, evidenced by the restoration of aromatic C=C bonding, a decrease in interlayer spacing, and sheet-like morphology. Mechanical testing revealed that increasing graphene content significantly enhanced the compressive and tensile strength of the composites. Ballistic testing using a 0.22-caliber firearm demonstrated that polyurethane composites containing ≥ 1.0 wt% rGO effectively resisted projectile penetration, whereas neat polyurethane and composites with lower graphene content were fully penetrated. These results demonstrate that graphite-derived graphene can substantially improve the mechanical integrity and ballistic resistance of polyurethane composites, highlighting its potential as a candidate material for lightweight personal protection systems.

1. INTRODUCTION

Graphene is a two-dimensional material composed of carbon atoms arranged in a hexagonal lattice [1]. The two-dimensional structure and covalent bonding of graphene endow it with excellent electrical, thermal, and mechanical properties [2]. Strong covalent C–C bonds make graphene difficult to deform, giving it a Young's modulus of up to 1.1 TPa [3]. Graphene can exhibit a tensile strength up to ~100 times that of steel [4]. Graphene is lightweight due to its atomically thin structure. It can be produced from graphite via exfoliation/chemical routes [5].

Graphite exhibits several properties: it is black, electrically conductive, heat-resistant, soft, slippery, and insoluble in water and organic solvents [6]. Graphite consists of hexagonally arranged carbon atoms, analogous to fused benzene rings without hydrogen atoms [7]. Graphite is widely produced and sold commercially at relatively low prices. Commercial graphite is abundant, yet its high-value utilization remains limited [8].

Although graphite is inexpensive and abundant, it does not readily exfoliate into single-layer graphene sheets [9].

In ballistic protection applications, materials are required not only to exhibit high strength but also to effectively absorb and dissipate the kinetic energy generated by high-velocity impacts. Graphene has emerged as a promising reinforcing material for ballistic composites owing to its exceptional elastic modulus, high aspect ratio, and two-dimensional layered structure. Under impact loading, graphene can enhance energy absorption through several mechanisms, including crack deflection and suppression of crack propagation, lamellar exfoliation or interlayer sliding between graphene sheets, and efficient stress transfer from the polymer matrix to the graphene layers. These mechanisms promote stress redistribution, reduce localized stress concentration, and facilitate large-area plastic deformation of the matrix, thereby improving impact and penetration resistance in graphene-reinforced polymer composites.

In ballistic impact conditions, effective protective materials must dissipate high kinetic energy through mechanisms such as crack deflection, interfacial debonding, stress transfer, and plastic deformation of the matrix. Graphene has been reported to enhance energy absorption through its exceptional stiffness, high aspect ratio, and layered structure, enabling load transfer and crack-arrest mechanisms within polymer matrices. However, most previous studies have focused on graphene derived from high-purity graphite or chemical vapor deposition routes, while systematic investigations on graphene

synthesized from commercially available graphite and its application in ballistic polyurethane composites remain limited.

The synthesis method of graphite into graphene is carried out by a chemical process known as the Hummers method [10]. This process oxidizes graphite to graphene oxide (GO), which can then be exfoliated and reduced to yield graphene-based powders. The modified Hummers method is practical and scalable for producing GO, which can be subsequently reduced to rGO [11]. Graphite powder is first oxidized to graphite oxide, which is then exfoliated to produce GO [12]. The GO obtained via the process of exfoliating graphite oxide layers was carried out by sonication [13]. The resulting GO is then chemically reduced to remove oxygen-containing functional groups, yielding reduced graphene oxide (rGO) with a more graphitic structure [14].

Research on the synthesis of graphene from commercial graphite so far is still lacking. Commercial graphite is widely available and could serve as a low-cost precursor for graphene-based reinforcements in lightweight structural composites.

Therefore, this study aims to synthesize graphene from commercial graphite using a chemical exfoliation–reduction route, systematically characterize the structural evolution from graphite to graphene, and evaluate the effect of graphene content on the mechanical and ballistic performance of graphene–polyurethane composite materials.

2. MATERIALS AND METHODS

Materials used in this research included commercial graphite, polyurethane resin, sodium nitrate ($NaNO_3$) p.a, sulfuric acid (H_2SO_4) 98% p.a, potassium permanganate ($KMnO_4$) p.a, hydrogen peroxide (H_2O_2) 30% p.a, barium sulfate ($BaSO_4$) p.a, barium chloride ($BaCl_2$) p.a, hydrochloric acid (HCl) 35% p.a, Zn powder, ice pack, filter paper, and distilled water. Instruments used in this research were a Scanning Electron Microscope (SEM), X-Ray Diffraction (XRD), Fourier Transform Infrared (FTIR), a series of refrigeration equipment, ovens, magnetic stirrers, an analytical balance, ultrasonic, centrifuge, and standard laboratory glassware.

2.1 Synthesis of graphite oxides

Commercial graphite was mixed with 80 mL of 98% H_2SO_4 and 4 g of $NaNO_3$, and stirred magnetically for 4 h while maintaining the temperature below 20 ℃. After stirring for 2 hours, 8 g $KMnO_4$ was added gradually and continued stirring for 4 hours, until the mixture changes color from dark green to purplish to dark brown, accompanied by the release of NOx gas. After 4 hours, continue stirring for another 24 hours at 35 ℃ to ensure complete oxidation. Next, 200 mL of distilled water was added slowly, followed by stirring for 1 h. Distilled water was added slowly under cooling, followed by H_2O_2 addition to quench residual permanganate until the slurry turned bright yellow. The resulting suspension was centrifuged and washing was continued until no sulfate ions were detected in the supernatant using $BaCl_2$ solution (no $BaSO_4$ precipitate). The graphite oxide product was then dried at 110 ℃ for 12 h [15].

The synthesis of graphite oxide yielded approximately 76.52% relative to the initial graphite mass, indicating efficient oxidation under the modified Hummers method.

2.2 Synthesis of reduced graphene oxide

As much as 40 mg graphite oxide dispersed in distilled water with a concentration of 1 mg/mL, it is sonicated for 120 minutes to obtain GO [15]. The conversion of graphite oxide to GO resulted in a yield of approximately 73.47%, suggesting minimal material loss during purification and washing processes.

As much as 40 mg GO is reduced by adding 2.4 g Zn and 10 mL HCl 35% and stirring for one hour. Next, 10 ml of 35% HCl was added to reduce the remaining Zn. The reduced graphene was then neutralized to a pH by washing with distilled water several times and was heated in the furnace at 200 ℃ for 12 hours [15]. The chemical reduction process produced graphene with an overall yield of approximately 55.57%, calculated based on the mass of dried graphene relative to the starting GO. The gradual decrease in yield from oxidation to reduction stages is attributed to the removal of oxygen-containing functional groups and elimination of residual impurities during successive purification steps.

2.3 Preparation of graphene–polyurethane composites

Graphene with varying concentrations of 0.25%; 0.5%; 0.75%; 1% and 1.5% of the weight of polyurethane was dispersed into Shore D polyurethane resin, which is a polyurethane resin that has the highest strength and hardness level, then homogenized with an ultrasonic tip. Ultrasonic dispersion was performed using a probe-type ultrasonic homogenizer operated at a frequency of 20 kHz. The stirring and homogenization process was carried out for varying times of 2 hours, 3 hours, and 4 hours, then a resin hardener was added with a ratio of 1:1. Stirred with a metal stirrer until mixed homogeneously, then inserted into the mold until hardened. The graphene-polyurethane composite layer was then tested for its potential as a bulletproof vest material.

2.4 Characterization by Fourier Transform Infrared

This characterization used FTIR with a wavenumber range of 400-4000 cm^{-1} with a KBr pellet, the baseline method [16].

2.5 Characterization with X-Ray Diffraction

XRD testing was carried out with a variety of 5-80° with an interval of 0.02°/step and Cu Kα radiation (λ = 1.5406 Å) [17].

2.6 Characterization with Scanning Electron Microscope-Energy Dispersive X-Ray

The Scanning Electron Microscope-Energy Dispersive X-Ray (SEM-EDX) test was carried out to determine the surface morphology and content of the elements in the sample, using SEM-EDX machines with a voltage of 20 kV [18].

2.7 Compressive strength evaluations

Compressive tests were conducted at a constant crosshead speed of 1.3 mm/min in accordance with ASTM D695 to evaluate the compressive strength of the graphene–polyurethane composites.

A compressive strength test is a test that aims to determine the strength of a material, so that an overview of the mechanical properties of a material is known. Graphene–

polyurethane composites that have been in the form of slabs with a length of 60 mm, a width of 60 mm, and a thickness of 17 mm were tested using UTM/Compression Fixture, Specimen Dimensions Conform to D695 with various variations in graphene and polyurethane concentrations without the addition of graphene [19].

2.8 Tensile strength evaluations

Tensile tests were performed using a Universal Testing Machine (UTM) at a loading rate of 5 mm/min following ASTM D638 to determine the tensile properties of the graphene–polyurethane composites.

Tensile strength evaluations are a test of materials to determine the characteristics and mechanical properties of materials, especially strength and resistance to tensile loads. Graphene–polyurethane composite material is formed with a length of 165 mm, a width of 20 mm, and a thickness of 16 mm. Furthermore, tests were carried out with a UTM on graphene–polyurethane composites with various variations in graphene and polyurethane concentrations without the addition of graphene [19].

2.9 Ballistic testing

Ballistic testing was conducted based on the NIJ Standard-0101.06 protocol using a modified experimental setup with a firing distance of 5 m. The projectile used in this study was a 0.22-caliber round-nose lead bullet with a measured mass of 2.6 g. The initial velocity of the projectile was approximately 370 m/s, based on firearm specifications for the ammunition used. Based on these values, the corresponding kinetic energy of the projectile was calculated using $E = ½ mv^2$, yielding an impact energy of approximately 178 J. The ballistic tests were performed using a Walther 0.22-caliber pistol at the "Tunggal Panaluan" shooting range of the South Sulawesi Police Brimob Unit [20]. Ballistic tests were carried out on polyurethane without the addition of graphene and on graphene-polyurethane composites that had been varied. The concentration of graphene addition was 0.25%; 0.5%; 0.75%; 1%; and 1.5%, so that data was obtained to withstand bullet projectile fire.

3. RESULTS AND DISCUSSION

3.1 Characterization with Fourier Transform Infrared

Testing with FTIR was carried out to determine the functional groups formed during the synthesis process, with a wavelength range of 400-4000 cm^{-1} by the baseline method. The FTIR spectrum results of the sample are shown in Figure 1.

Figure 1 shows the absorption at a wavenumber of 1600 cm^{-1}, showing the presence of aromatic C=C bonds, which is an indication of the formation of graphene [21]. The FTIR spectrum of graphite shows minimal absorption features, reflecting its highly ordered sp^2 carbon structure with the absence of oxygen-containing functional groups. After oxidation, several new absorption bands appear, indicating the successful introduction of oxygen functionalities into the carbon framework. The broad band observed around 3400 cm^{-1} corresponds to O–H stretching vibrations, suggesting the presence of hydroxyl groups and adsorbed water molecules. The strong absorption at approximately 1720 cm^{-1} is assigned to C=O stretching vibrations, while the band near 1050–1250 cm^{-1} corresponds to C–O stretching vibrations. These features confirm the effective oxidation of graphite into graphite oxide and GO.

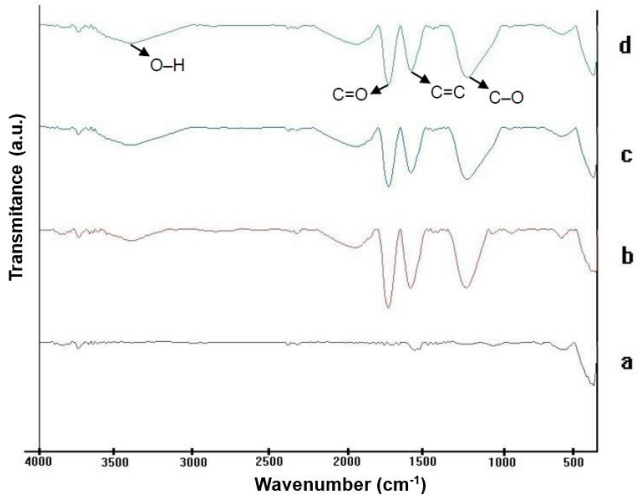

Figure 1. Comparison of FTIR spectrum results on graphite, graphite oxide, graphene oxide (GO), and graphene samples

Following the reduction process (Figure 1), a pronounced decrease in the intensity of oxygen-related absorption bands is observed. The O–H stretching band around 3400 cm^{-1} becomes significantly weaker, indicating the removal of hydroxyl groups and interlayer water molecules. Similarly, the marked attenuation of the C=O and C–O absorption bands demonstrates the successful reduction and elimination of oxygen-containing functional groups. Concurrently, the absorption band around 1600 cm^{-1}, associated with aromatic C=C stretching vibrations, becomes more prominent, suggesting the partial restoration of the conjugated sp^2 carbon network.

The reduction of oxygen-containing functional groups has important structural and interfacial implications. The removal of polar groups leads to a more compact and hydrophobic carbon structure, which facilitates closer contact between graphene layers and enhances π–π interactions. In composite systems, these changes are expected to improve interfacial bonding between reduced graphene and the matrix, thereby contributing to enhanced mechanical integrity and functional performance. Overall, the FTIR results confirm the success of the reduction process and provide chemical evidence supporting the structural reorganization of graphene.

3.2 Characterization with X-Ray Diffraction

They are testing using XRD aimed at determining the crystal phase of graphite, graphite oxide, GO, and graphene. The analysis was conducted with an angle range of 2θ between 5–80° and a wavelength of 1.5 Å. Graphite and graphite oxide have a 2θ band at around 26°, while GO and graphene have a 2θ band around 23° [22].

XRD analysis was conducted to examine the structural changes of graphite (a), graphite oxide (b), GO (c), and reduced graphene (d), as shown in Figure 2. Pristine graphite exhibits a sharp diffraction peak at $2\theta \approx 25.21°$, corresponding to the (002) plane, indicating a well-ordered graphitic structure. After oxidation, this peak shifts to lower angles (2θ

≈ 24.84°), reflecting an increase in interlayer spacing due to the introduction of oxygen-containing functional groups.

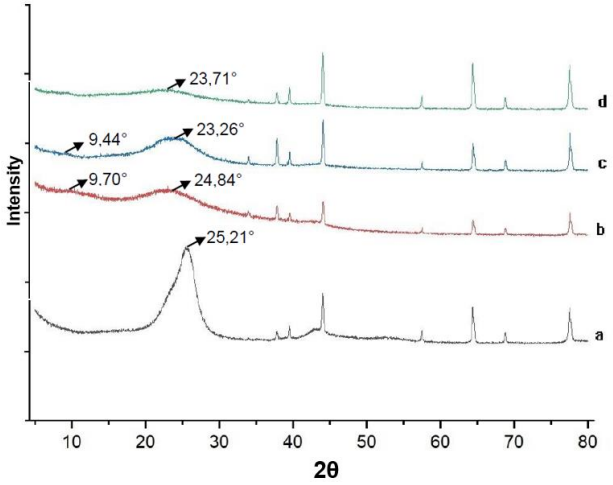

Figure 2. Comparison of X-Ray Diffraction (XRD) spectrum results on graphite, graphite oxide, graphene oxide (GO), and graphene samples

GO shows a characteristic low-angle diffraction peak at 2θ ≈ 9.44°, corresponding to the (001) plane, which indicates a significant expansion of interlayer spacing caused by extensive oxidation and intercalation of oxygen groups and water molecules. Following reduction, the disappearance of this low-angle peak and the appearance of a broad peak at 2θ ≈ 23.71° confirm the effective removal of oxygen-containing groups and the contraction of interlayer spacing. This shift suggests partial restoration of the sp^2 carbon structure with a more disordered stacking arrangement.

The contraction of interlayer spacing observed in XRD is consistent with the reduction of oxygen-containing functional groups identified by FTIR analysis. These structural changes enhance layer-to-layer contact and are expected to improve interfacial bonding in composite materials, confirming the success of the reduction process.

The difference between the amorphous and crystalline phases can be seen from the diffractogram form on XRD. The diffractogram pattern, which tends to widen, shows the amorphous phase, while the sharply shaped diffractogram pattern shows the crystalline phase [23]. Based on the diffractogram in Figure 2, the graphene obtained has an amorphous phase.

3.3 Characterization with Scanning Electron Microscope-Energy Dispersive X-Ray

The SEM-EDX is used to determine the surface morphological structure and elemental content of the samples tested. The morphology of graphene is in the form of thin sheets, analyzed by using SEM-EDX [21]. The surface morphology of graphite, graphite oxide, GO, and graphene is shown in Figure 3 using SEM-EDX.

Based on Figure 3, the surface morphology structure of the graph looks like rough chunks. Furthermore, the morphological structure of graphite oxide is in the form of smaller fragments. In GO, the presence is in the form of coarse and folded sheets, while in graphene, the presence is of larger sheets. Graphene appears to consist of one layer and is hexagonal. Testing the element content in the sample can be done using SEM-EDX [24]. The results of the comparison prove the element content against graphite, graphite oxide, GO, and graphene, as shown in Table 1.

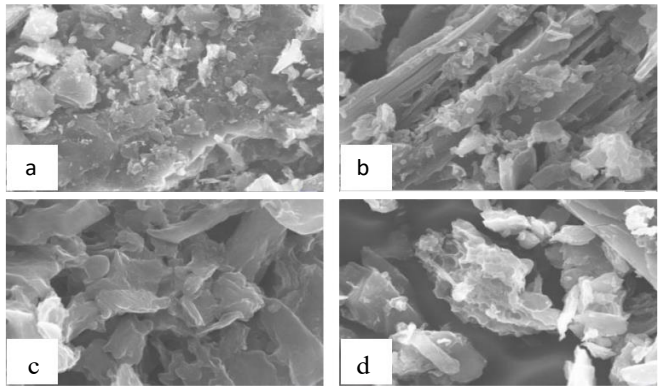

Figure 3. Results of surface morphology test with Scanning Electron Microscope-Energy Dispersive X-Ray (SEM-EDX) (a) graphite, (b) graphite oxide, (c) graphene oxide (GO), and (d) graphene

Table 1. Comparison of element contents tested using SEM-EDX on graphite, graphite oxide, graphene oxide (GO), and graphene samples

Element	Graphite	Graphite Oxide	Graphene Oxide	Graphene
Carbon	92.29	62.23	66.24	69.61
Nitrogen	3.07	-	-	-
Oxygen	2.08	36.86	33.18	28.09
Aluminum	0.15	0.22	0.04	0.27
Silicon	0.15	0.09	-	0.47
Sulphur	1.31	0.42	0.27	0.21
Iron	0.24	-	-	-
Potassium	-	0.19	0.27	0.12
Zinc	-	-	-	1.24

Based on Table 1, graphite has elements in the form of aluminum, silicon, sulfur, and iron, which can affect the synthesis process into graphene. Table 1 shows that Zn is still found in graphene samples, this showed that the reduction process was still not perfect. Although residual Zn is detected by EDX analysis, its low intensity and homogeneous distribution suggest that it does not significantly alter the composite microstructure. No evidence of Zn-rich agglomeration or secondary brittle phases is observed in the SEM images. Nevertheless, excessive Zn content could potentially lead to embrittlement, and therefore, controlled Zn loading remains an important consideration for optimizing composite performance.

3.4 Compressive strength testing with hammers test

The compressive strength test is a test that aims to determine the hardness of a material, so that the description of the mechanical properties of a material is known. This test is based on the emphasis of a certain compressive force on the material [19]. Strankowski et al. [25] reported that the addition of a concentration of 0.5% GO can increase the mechanical strength of polyurethane by 17%. The test was carried out by making variations in graphene concentrations. In polyurethane (without graphene) and the addition of graphene with a concentration of 0.25%; 0.5%; 0.75%; 1%; and 1.5%. This was conducted to determine the effect of graphene concentration on the strength of graphene-polyurethane

composites.

The results show that the higher the concentration of graphene in the graphene-polyurethane composite material, the higher the hardness level of the graphene-polyurethane composite. The research data can be seen in Figure 4.

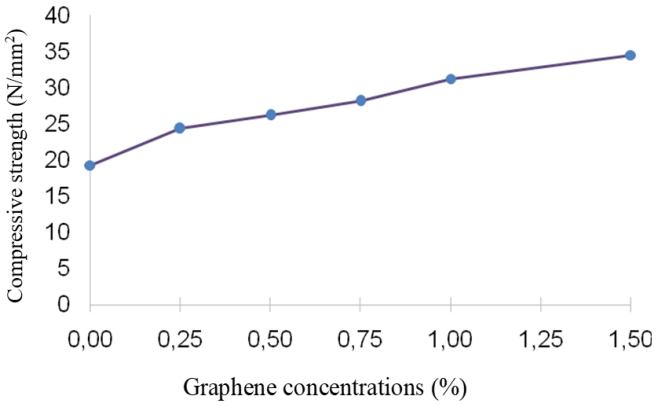

Figure 4. Graphene concentration effect on compressive strength

3.5 Tensile strength test with Universal Testing Machine

The tensile strength test is a test of materials to determine the characteristics and mechanical properties of materials, especially strength and resistance to tensile loads [20]. To test the tensile strength, graphene-polyurethane composite materials were made several variations based on the concentration level of the composited graphene which was 0.25%; 0.5%; 0.75%; 1%; 1.5%; and in polyurethane without graphene as a control. This aims to determine the effect of graphene concentration level on the strength and resistance of graphene-polyurethane composite materials to tensile loads. The results of the study show that the higher the concentration of graphene composited in graphene–polyurethane, the strength and durability also increase. The research data can be seen in Figure 5.

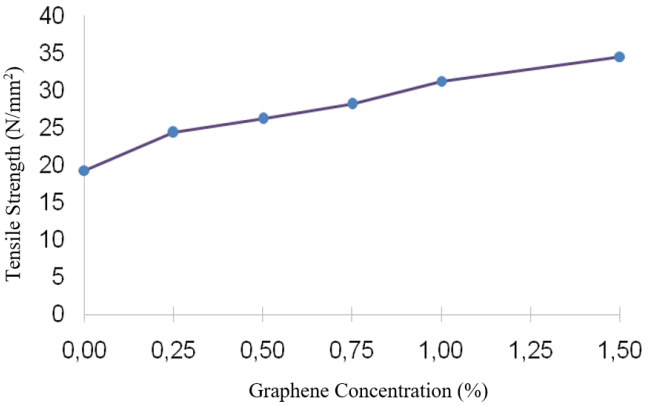

Figure 5. The effect of graphene concentrations on tensile strength

The improvement in composite performance with increasing graphene content, as shown in Figures 4 and 5, can be explained by composite reinforcement mechanisms rather than a simple "higher is better" trend. At low graphene loadings, graphene sheets are well dispersed within the matrix, enabling effective stress transfer from the matrix to the high-modulus graphene through strong interfacial interactions. This load transfer mechanism allows graphene to act as an efficient reinforcing phase, resulting in enhanced mechanical performance.

In addition to load transfer, graphene contributes to crack propagation resistance by acting as a crack deflector and crack-bridging agent. The presence of graphene sheets forces propagating cracks to follow more tortuous paths, thereby increasing the energy required for fracture and delaying crack growth. This mechanism further contributes to the observed improvement in composite properties.

A pronounced enhancement is observed at an optimal graphene content of approximately 1%, which is attributed to a balance between sufficient filler content and good dispersibility. At this concentration, graphene forms an effective reinforcement network without significant agglomeration. At higher loadings, however, graphene sheets tend to agglomerate due to strong van der Waals interactions, leading to stress concentration sites and reduced interfacial efficiency. Consequently, the reinforcing effect does not increase proportionally beyond the optimal concentration.

3.6 Ballistic testing

Applications of graphene–polyurethane composite materials will be used as bulletproof vests. Therefore, ballistic or firing tests are carried out to determine the potential of graphene-polyurethane composites as bulletproof vest materials. As a comparison material, polyurethane without graphene and graphene composite materials – polyurethane made a variation in graphene concentration of 0.25%; 0,5%; 0,75%; 1%; and 1.5% as done on the compressive and tensile strength testing of composite materials. In addition, the thickness of the samples/composite materials is made with a relatively similar size of ± 17 mm. The type of test weapon used is also the same, namely the Short Barrel Type (Pistol), caliber 0.22 inches of the Walter Brand, made in Germany, the type of round-nose sharp bullet ammunition made of lead antimony projectile material, speed Bullet fire ± 370 m/s. Then the firing range is carried out as far as 5 m in accordance with international standards for ballistic tests [20]. These things aim to obtain accurate data. The test results obtained show that the level of graphene concentration affects the strength of the graphene–polyurethane composite material against the impact of the bullet projectile, that is, the higher the concentration, the stronger the resistance to the impact of the projectile of the firearm bullet. The research data can be seen in Table 2.

Table 2. Comparative data of polyurethane materials without graphene and graphene-polyurethane composites

Sample (%)	Sample Thickness (mm)	Firing Distance (m)	Result	Information
Polyurethane	17.26	5	Break	Pierce
0.25	17.27	5	Break	Pierce
0.5	17.29	5	Break	Pierce
0.75	17.32	5	Break	Pierce
1	17.33	5	Un broken	Impenetrable
1.5	17.41	5	Un broken	Impenetrable

The research data shows that polyurethane materials without graphene and graphene-polyurethane composites with a graphene addition concentration of 0.25% to 0.75% are obtained from breaking and penetrating by bullet projectiles,

while graphene concentrations of 1% to 1.5% are obtained as non-breaking and non-penetrating results. Although the 1.5 wt% composite also prevented penetration, the 1 wt% graphene content was considered optimal due to its balance between ballistic performance, dispersion quality, and material processability. At higher graphene loadings, increased filler–filler interactions may promote agglomeration, which can reduce dispersion uniformity and adversely affect composite processability without providing a proportional improvement in ballistic resistance. These results are also in line with the results of the hardness and tensile strength tests of composite materials. It can therefore be concluded that the concentration of graphene is more than 1%. It is the right concentration or suitable for application as a bulletproof vest made of graphene–polyurethane composite material. The results of the ballistic test can be seen in Figure 6. In polyurethane without the addition of graphene and in polyurethane graphene composites with graphene addition concentrations of 0.25% to 0.75%, graphene-polyurethane composites were seen to break with irregular shapes, due to collisions with bullet projectiles from pistol guns at high speed. However, at concentrations of 1% and 1.5%, the graphene-polyurethane composite is able to withstand impact so that it is not penetrated by bullet projectiles.

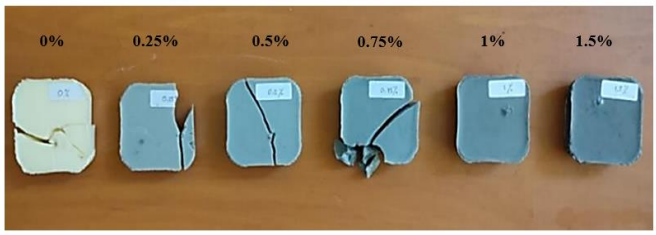

Figure 6. The ballistic test results

At a graphene addition concentration of 1%, the shot marks on the graphene-polyurethane composite are more obvious and rough, as shown in Figure 7, while at a graphene addition concentration of 1.5%, it looks smoother as seen in Figure 8. This proves that the more graphene concentrations are added to the graphene-polyurethane composites up to 1.5%, the strength of the composite will also increase.

Figure 7. Ballistic test results at 1% concentration

The enhanced impact resistance observed in graphene-reinforced composites can be explained by multiple energy dissipation mechanisms operating during ballistic impact. Upon impact, graphene sheets initially participate in load bearing and undergo self-fracture, which consumes a portion of the incident kinetic energy. Simultaneously, interlaminar sliding between graphene layers and the surrounding matrix occurs, promoting frictional energy dissipation and delaying crack propagation.

Figure 8. Ballistic test results at 1.5% concentration

In addition to these localized mechanisms, graphene promotes large-area deformation of the matrix by redistributing stress away from the impact point. This stress delocalization enables the matrix to deform plastically over a wider region, thereby increasing the overall energy absorption capacity of the composite. For samples that are not penetrated, the dominant damage modes include matrix cracking, interfacial debonding, and limited delamination, rather than catastrophic fracture. These damage modes indicate effective energy dissipation and structural integrity retention during impact loading.

4. CONCLUSIONS

Graphene was successfully synthesized from commercial graphite and effectively incorporated into a polyurethane matrix. Structural characterization confirmed the reduction of GO and the formation of layered graphene structures. Mechanical testing demonstrated significant improvements in compressive and tensile strength with increasing graphene content. Most importantly, ballistic testing revealed that graphene – polyurethane composites containing ≥ 1 wt% graphene were capable of resisting projectile penetration, while lower concentrations and neat polyurethane failed under identical conditions. Despite these promising results, this study is limited by the presence of residual Zn from the reduction process, potential graphene agglomeration, and the use of low-caliber firearms. Future work should focus on optimizing graphene dispersion, eliminating metallic residues, and evaluating ballistic performance under higher-velocity impact conditions and different polymer matrices.

ACKNOWLEDGMENT

The authors are grateful for the financial support provided by the Ministry of Research, Technology, and Higher Education.

REFERENCES

[1] Neto, A.H.C., Guinea, F., Peres, N.M.R., Novoselov, K.S., Geim, A.K. (2009). The electronic properties of

graphene. Reviews of Modern Physics, 81: 109-162. https://doi.org/10.1103/RevModPhys.81.109
[2] Dimiev, A.M., Eigler, S. (2017). Graphene Oxide: Fundamentals and Applications. Mechanical Industry Press.
[3] Lee, C., Wei, X., Kysar, J.W., Hone, J. (2008). Measurement of the elastic properties and intrinsic strength of monolayer graphene. Science, 321(5887): 385-388. https://doi.org/10.1126/science.1157996
[4] Das, D.K., Swain, P.K., Sahoo, S. (2016). Graphene in turbine blades. Modern Physics Letters B, 30(20): 1650262. https://doi.org/10.1142/S0217984916502626
[5] Erik, H. (2010). The Nobel Prize in Physics 2010 Stockholm. The Royal Swedish Academy of Sciences.
[6] Cermak, M., Perez, N., Collins, M., Bahrami, M. (2020). Material properties and structure of natural graphite sheet. Scientific Reports, 10(1): 18672. https://doi.org/10.1038/s41598-020-75393-y
[7] Liu, G., Chen, X.Q., Liu, B., Ren, W., Cheng, H.M. (2020). Six-membered-ring inorganic materials: Definition and prospects. National Science Review, 8(1): nwaa248. https://doi.org/10.1093/nsr/nwaa248
[8] Dresselhaus, M.S., Dresselhaus, G. (2002). Intercalation compounds of graphite. Advances in Physics, 51(1): 1-186. https://doi.org/10.1080/00018730110113644
[9] Li, J., Zeng, X., Ren, T., Van der Heide, E. (2014). The preparation of graphene oxide and its derivatives and their application in bio-tribological systems. Lubricants, 2(3): 137-161. https://doi.org/10.3390/lubricants2030137
[10] Marcano, D.C., Kosynkin, D.V., Berlin, J.M., Sinitskii, A., et al. (2018). Correction to improved synthesis of graphene oxide. Acs Nano, 12(2): 2078-2078. https://doi.org/10.1021/acsnano.8b00128
[11] Emiru, T.F, Ayele, D.W. (2017). Controlled synthesis, characterization and reduction of graphene oxide: A convenient method for large scale production. Egyptian Journal of Basic and Applied Sciences, 4(1): 74-79. https://doi.org/10.1016/j.ejbas.2016.11.002
[12] Li, X., Liang, X., Wang, Y., Wang, D., Teng, M., Xu, H., Zhao, B., Han, L. (2022). Graphene-based nanomaterials for dental applications: Principles, current advances, and future Outlook. Frontiers in Bioengineering and Biotechnology, 10: 804201. https://doi.org/10.3389/fbioe.2022.804201
[13] Tariq, W., Ali, F., Arslan, C., Nasir, A., Gillani, S.H., Rehman, A. (2022). Synthesis and applications of graphene and graphene-based nanocomposites: Conventional to artificial intelligence approaches. Frontiers in Environmental Chemistry, 8: 890408. https://doi.org/10.3389/fenvc.2022.890408
[14] Mohammedture, M., Rajput, N., Perez-Jimenez, A.I. (2023). Impact of probe sonication and sulfuric acid pretreatment on graphene exfoliation in water. Scientific Reports, 13(1): 18523. https://doi.org/10.1038/s41598-023-45874-x
[15] Azizighannad, S., Mitra, S. (2018). Stepwise reduction of graphene oxide (GO) and its effects on chemical and colloidal properties. Scientific Reports, 8(1): 10083. https://doi.org/10.1038/s41598-018-28353-6
[16] Khadifah, F.M., Nurisal, R. (2017). Graphene synthesis based on coconut shell charcoal using the modified hummers method. Doctoral dissertation, Institut Teknologi Sepuluh Nopember, Surabaya, Indonesia. https://www.semanticscholar.org/paper/Sintesis-Graphene-Berbasis-Arang-Tempurung-Kelapa-Khadifah-Nurisal/3cc785f9797bf7c8503cc40f6117930dc356d80c.
[17] Gascho, J.L., Costa, S.F., Recco, A.A., Pezzin, S.H. (2019). Graphene oxide films obtained by vacuum filtration: X-ray diffraction evidence of crystalline reorganization. Journal of nanomaterials, 2019(1): 5963148. https://doi.org/10.1155/2019/5963148
[18] Park, J.B., Kim, Y.J., Kim, S.M., Yoo, J.M., et al. (2016). Non-destructive electron microscopy imaging and analysis of biological samples with graphene coating. 2D Materials, 3(4): 045004. https://doi.org/ 10.1088/2053-1583/3/4/045004
[19] Xie, W.Q., Liu, X.L., Zhang, X.P, Liu, Q.S., Wang, E.Z. (2025). A review of test methods for uniaxial compressive strength of rocks: Theory, apparatus and data processing. Journal of Rock Mechanics and Geotechnical Engineering, 17(3): 1889-1905. https://doi.org/10.1016/j.jrmge.2024.05.003
[20] Morăraș, C.I., Husaru, D., Goanță, V., Bârsănescu, P.D., Lupu, F.C., Munteanu, C., Cimpoesu, N., Cosau, E.R. (2024). A new method for compression testing of reinforced polymers. Polymers, 16(21): 3071. https://doi.org/10.3390/polym16213071
[21] Azizah, L.N., Susanti, D. (2014). The effect of variations in Zn content and hydrothermal temperature on the structure and electrical conductivity of graphene material. Jurnal Teknik ITS, 3(2): F209-F214. https://doi.org/10.12962/j23373539.v3i2.6620
[22] Taufantri, Y., Irdhawati, I., Asih, I.A.R.A. (2016). Sintesis dan karakterisasi grafena dengan metode reduksi grafit oksida menggunakan pereduksi Zn. Jurnal Kimia Valensi, 2(1): 17-23. https://doi.org/10.15408/jkv.v2i1.2233
[23] Hidayat, A., Setiadji, S., Hadisantoso, E.P. (2018). Sintesis oksida grafena tereduksi (rGO) dari arang tempurung kelapa (Cocos nucifera). Al Kimiya: Jurnal Ilmu Kimia dan Terapan, 5(2): 68-73.
[24] Siburian, R., Sihotang, H., Raja, S.L., Supeno, M., Simanjuntak, C. (2018). New route to synthesize of graphene nano sheets. Oriental Journal of Chemistry, 34(1): 182-187. https://doi.org/10.13005/ojc/340120
[25] Strankowski, M., Włodarczyk, D., Piszczyk, Ł., Strankowska, J. (2016). Polyurethane Nanocomposites Containing Reduced Graphene Oxide, FTIR, Raman, and XRD Studies. Journal of Spectroscopy, 2016: 7520741. https://doi.org/10.1155/2016/7520741